

# Limit on the Role of Activity in Controlling the Release-Ready Supply of Synaptic Vesicles

John F. Wesseling and Donald C. Lo

Department of Neurobiology, Duke University Medical Center, Durham, North Carolina 27710

Typical fast chemical synapses in the brain weaken transiently during normal high-frequency use after expending their presynaptic supply of release-ready vesicles. Although it takes several seconds for the readily releasable pool (RRP) to refill during periods of rest, it has been suggested that the replenishment process may be orders of magnitude faster when synapses are active. Here, we measure this replenishment rate at active Schaffer collateral terminals by determining the maximum rate of release that can still be elicited when the RRP is almost completely exhausted. On average, we find that spent vesicles are replaced at a maximum unitary rate of 0.24/sec during periods of intense activity. Because the replenishment rate is

similar during subsequent periods of rest, we conclude that no special mechanism accelerates the mobilization of neurotransmitter in active terminals beyond the previously reported, several-fold, residual calcium-driven modulation that persists for several seconds after bouts of intense synaptic activity. In the course of this analysis, we provide new evidence supporting the hypothesis that a simple enzymatic step limits the rate at which reserve synaptic vesicles become ready to undergo exocytosis.

*Key words:* synaptic physiology; presynaptic; synaptic vesicle; priming; short-term plasticity; readily releasable pool

Recently there has been considerable interest in measuring the time required for reserve synaptic vesicles to become available to participate in neurotransmission at CNS synapses (Stevens and Tsujimoto, 1995; Rosenmund and Stevens, 1996; Dobrunz and Stevens, 1997; Stevens and Wesseling, 1998; Wu and Borst, 1999; Pyle et al., 2000). This work is important because a complete picture of the molecular basis of synaptic function requires a clear understanding of the kinetics of the various steps in the synaptic vesicle cycle, in addition to the identification of the enzymes involved. It is also important from a computational perspective, because the rate at which vesicles become ready to participate in synaptic transmission is a key element that determines the means by which information can be transferred between neurons via synapses.

Typical presynaptic terminals contain hundreds of vesicles loaded with chemical transmitter, but at any given time, only a few of them are functionally available to be released quickly (Schikorski and Stevens, 1997, 2001). This release-ready subset of synaptic vesicles constitutes the readily releasable pool (RRP). When their RRP is empty during episodes of heavy use, synapses exhibit short-term depression, transiently becoming less reliable at transmitting information because they can no longer consistently provide neurotransmitter for intercellular signaling (Elmqvist and Quastel, 1965; Rosenmund and Stevens, 1996).

Previous studies have primarily measured the time it takes for the RRP to refill during periods of rest, most finding that recovery from depletion takes at least several seconds (Birks and MacIn-

tosh, 1961; Elmqvist and Quastel, 1965; Stevens and Tsujimoto, 1995; Rosenmund and Stevens, 1996; Wu and Borst, 1999). The residual calcium that is cleared slowly from synaptic terminals after bouts of intense activity has been shown to accelerate the replenishment process several-fold (Dittman and Regehr, 1998; Stevens and Wesseling, 1998, 1999a; Wang and Kaczmarek, 1998). In those studies, however, the replenishment rate was monitored only during rest intervals that followed active episodes. It has been suggested that there may be an additional, qualitatively different activity-dependent mechanism that can accelerate the rate at which neurotransmitter becomes available for release to a much greater extent during periods of intense presynaptic activity (Kusano and Landau, 1975), perhaps via a rapid refilling of the spent release-ready vesicles themselves (Pyle et al., 2000).

In this study we examined the extent to which the RRP replenishment rate can be accelerated to counteract short-term depression during heavy synaptic use. Using stimulation protocols that were sufficient to drive the RRP of Schaffer collateral synapses into a near-empty steady state, we found that neurotransmitter becomes available for release only approximately two or three times as quickly when these synapses are active as it does during periods of rest, as predicted from the residual calcium-dependent type of replenishment-rate acceleration that has been reported previously (Stevens and Wesseling, 1998). We thus conclude that there is no special mechanism that accelerates the preparation of neurotransmitter for release in active terminals beyond this type of modulation that persists for several seconds after bouts of repetitive activity.

## MATERIALS AND METHODS

All synaptic responses were measured from patch-clamped neurons held in whole-cell voltage-clamp mode.

*Preparation.* Experiments were performed on transverse slices prepared from the hippocampi of 2- to 3-week-old mice. Mice were anesthetized by inhalation of halothane and decapitated soon after the

Received July 24, 2002; revised Sept. 6, 2002; accepted Sept. 9, 2002.

Funding was provided by National Institutes of Health Grants NS10827 (J.F.W.) and NS32742 (D.C.L.) and the McKnight Endowment Fund (D.C.L.). We thank Dr. Dana Cohen, Dr. Isabel Pérez-Otaño, Dr. Iman Brivanlou, and Dr. Richard Aldrich for providing helpful suggestions.

Correspondence should be addressed to John F. Wesseling, Duke University Medical Center 3209, Duke University Department of Neurobiology, Durham, NC 27710. E-mail: wesseling@neuro.duke.edu.

Copyright © 2002 Society for Neuroscience 0270-6474/02/229708-13\$15.00/0

disappearance of reflexive reactions to tail and foot pinches. Brains were removed rapidly and bathed in a chilled solution that had most of the sodium ions replaced with sucrose (in mM): 230 sucrose, 1.25  $\text{NaH}_2\text{PO}_4$ , 26  $\text{NaHCO}_3$ , 10 glucose, 3.5 KCl, 2.6  $\text{MgCl}_2$ , and 1.3  $\text{CaCl}_2$ . The cerebellum and brain stem were dissected away, and 400- $\mu\text{m}$ -thick coronal slices of the remaining brain were cut using a vibrating microtome. Hippocampal segments were dissected free, and area CA3 was removed for all experiments except those in which recordings were made of antidromic action potentials. The hippocampal slices were then gently washed three or four times in the physiological recording solution containing (in mM): 120 NaCl, 1.25  $\text{NaH}_2\text{PO}_4$ , 26  $\text{NaHCO}_3$ , 10 glucose, 3.5 KCl, 2.6  $\text{CaCl}_2$ , 1.3  $\text{MgCl}_2$ , picrotoxin (50  $\mu\text{M}$ ), and D(-)APV (50  $\mu\text{M}$ ), except where indicated. Recording solutions were bubbled with a mixture of 95%  $\text{O}_2$  and 5%  $\text{CO}_2$  for at least 20 min before addition of  $\text{CaCl}_2$  and  $\text{MgCl}_2$ . The slices were maintained in an interface slice chamber and humidified with the same gas mixture for between 2 and 10 hr before being transferred to the submerged recording chamber.

**Recording.** Slices were submerged in the recording chamber with a nylon mesh affixed to a platinum anchor. The solution in the 0.5 ml recording chamber was exchanged 5–10 times per minute with continuously bubbled recording solution. Most recordings were performed using 3–5 M $\Omega$  pipettes, filled with saline containing (in mM): 130 Cs-gluconate, 5 CsCl, 5 NaCl, 2  $\text{MgCl}_2$ , 2 MgATP, 0.2 LiGTP, 1 EGTA, 0.2  $\text{CaCl}_2$ , and 10 HEPES. For experiments in which action potentials were fired antidromically, a solution containing (in mM) 140 K-gluconate, 9 NaCl, 1  $\text{MgCl}_2$ , 2 MgATP, 0.2 LiGTP, 1 EGTA, 0.2  $\text{CaCl}_2$ , and 10 HEPES was used instead. Intracellular solutions were adjusted to pH 7.2 and an osmolarity of 290 mOsm.

**Stimulation.** A monopolar silver/silver chloride electrode inserted into a glass pipette (tip diameter between 20 and 40  $\mu\text{m}$ ) and filled with recording solution was used for evoking action potentials in the Schaffer collaterals for all experiments presented here. EPSCs were evoked by up to 1 mA of current for 100  $\mu\text{sec}$ . The more commonly used bipolar electrodes made of tungsten transiently became substantially less effective at eliciting action potentials over the course of single trials and were deemed unsuitable for these experiments. The experiment summarized in Figure 1*B* provides a good test for whether a stimulating device introduces unanticipated errors into the sorts of experiments detailed here. Because small changes in stimulus intensity can lead to large changes in the number of axons stimulated (Allen and Stevens, 1994), we stress that it is not adequate to instead monitor only changes in the size of the electrical artifact associated with each stimulus.

Minimal stimulator settings (see Fig. 7) were determined during low-frequency stimulation as the strength needed to elicit successful synaptic transmission less than half of the time. To ensure that transmission failures did not result from nerve conduction failures arising from axonal threshold fluctuations, minimal intensities were used only if it was possible to both increase and decrease the stimulus intensity by several percentages without noticeably changing the probability of release.

**Drugs.** NBQX (3  $\mu\text{M}$ ) was added to block glutamatergic transmission for antidromic action potential recordings. Stock solutions of cyclothiazide (CTZ) (20 mM) were made in DMSO and used at final concentration of 100  $\mu\text{M}$  where indicated. Kynurenic acid (KYN) was added in powder form directly to the recording solution and then dissolved by vigorous stirring for several hours.

**Experimental design.** In general, it was often possible to repeat several trials of each experiment on individual preparations. To allow the synapses to recover completely between trials, at least 3 or 4 min was allowed for rest before high-frequency stimulation was initiated (4 min for most; 3 min for the minimal stimulation experiments). For the experiments documented in Figures 1*A*, 4, 5, 6, and 7, the experimental and control trials were alternated. The order of the different types of trials summarized in Figure 3 was shuffled. Data were accepted only if the access resistance was stationary throughout individual trials and also from trial to trial when the object was to compare synaptic response sizes between trials (see Figs. 1*A*, 4, 6, and 7).

**Analysis.** Synaptic size was measured as the slope of the rising phase of the postsynaptic response estimated by fitting the rising segment between 30 and 60% of the peak with a linear least squares fit. EPSCs recorded at  $\leq 20$  Hz were also measured as the current integral of the synaptic response to confirm that the relative measurements of short-term depression were accurate. Because typical synaptic responses took  $>25$  msec to decay, measurements of synaptic potentials recorded at 40 Hz were adjusted for the slope of the baseline response over the 5 msec that preceded the stimulus artifact ( $<15\%$  of total measure). For 20 Hz

stimulation, a similar correction did not contribute substantially to the measure. Because the rising phase of the smallest recordings made in 1000  $\mu\text{M}$  KYN were significantly contaminated by the stimulus artifact, the sizes of both the control and experimental recordings that involved this concentration of KYN were quantified as the current integral between 15 and 24 msec after the stimulus artifact.

## RESULTS

We studied the rate at which vesicular packets of transmitter become available for release at excitatory glutamatergic synapses between hippocampal Schaffer collaterals and the CA1 pyramidal neurons in transverse slice preparations. When long-term changes are blocked pharmacologically with NMDA receptor antagonists, activity does not affect the sensitivity of the postsynaptic receptors at these synapses; the size of the postsynaptic response elicited by the release of transmitter quanta stays constant during periods of intense use [Dobrunz and Stevens (1997); and see a series of control experiments presented below]. This allowed us to monitor the rate of transmitter release during Schaffer collateral stimulation with standard electrophysiological recordings of postsynaptic CA1 neurons.

### Sixty action potentials at 20 Hz exhaust the RRP

To measure the rate at which vesicles are prepared for exocytosis in active terminals, we developed a stimulation protocol that was sufficient to exhaust the RRP. Pilot experiments conducted on neurons grown in cell culture [similar to those described in Rosenmund and Stevens (1996)] indicated that 40 or fewer action potentials in a high-frequency train only partially emptied the RRP of those synapses, but that trains consisting of at least 60 action potentials were sufficient to completely exhaust the pools (data not shown).

Because the technique used in the cell culture system to check RRP fullness is not available in the slice preparation, an alternate test was devised that involved switching the frequency of stimulation during a repetitive train. Because readily releasable vesicles are functionally defined as the ones that are triggered for exocytosis directly by action potentials, increasing the stimulation rate when the RRP is still partially full should cause the rate of exocytosis to increase. Conversely, when the pool is empty, the synaptic strength is limited by the time it takes for fresh quanta of transmitter to become available for release, and that rate apparently does not change with stimulus frequency (Eccles and Rall, 1951; Curtis and Eccles, 1960; Elmqvist and Quastel, 1965; Abbott et al., 1997; Tsodyks and Markram, 1997; Stevens and Wesseling, 1998). We thus reasoned that if the RRP was left empty by a train of 60 action potentials, subsequently doubling the stimulation frequency would not change the overall rate of exocytosis.

Figure 1 shows that 60 action potentials fired at 20 Hz nearly completely empty the RRP of these synapses. Schaffer collaterals were stimulated 60 times at 20 Hz and then 21 more times either at 40 Hz or at 20 Hz as a control (Fig. 1*A*). During a brief settling time, the synaptic strength recorded at 40 Hz depressed quickly to one-half that recorded at 20 Hz (Fig. 1*A*, bottom versus top dashed lines). Because there were twice as many stimulations for each unit of time during the faster stimulation, the overall steady rate of release was the same at both frequencies. Thus, suddenly doubling the stimulus frequency to 40 Hz did not substantially increase the rate of transmitter release, suggesting that 60 action potentials at 20 Hz are sufficient to almost completely exhaust the RRP.

This logic is valid only if the stimulating apparatus successfully evoked action potentials in the same axons after each stimulus.

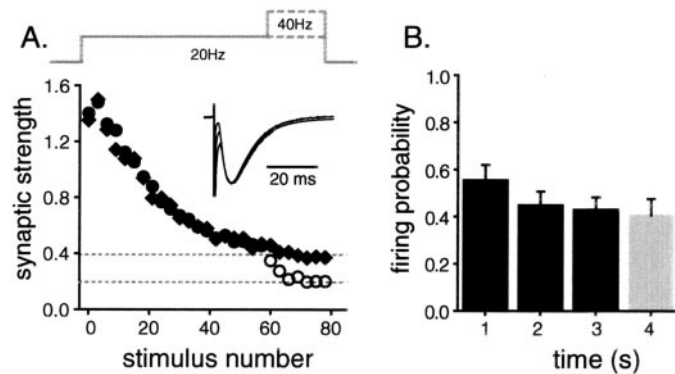


**Figure 1.** The RRP is emptied by 60 action potentials at 20 Hz. *A*, Schaffer collaterals were stimulated 60 times at 20 Hz and then 21 more times either at 40 or 20 Hz while postsynaptic responses were recorded by patch clamping CA1 pyramidal neuron somata. Fluctuations caused by the quantal nature of transmitter release, including frequent transmission failures, dominated the recordings during the 40 Hz stimulation, and so traces were averaged across all experiments before being measured (each point represents the average of 18 trials from 4 slices). The synaptic response sizes were binned in groups of three, normalized by the size of the first response, and plotted versus the stimulus number. *Diamonds* represent responses of synapses stimulated at 20 Hz throughout; *circles* are from trials where the frequency was doubled. The *filled circles* represent 20 Hz responses; the *open circles* are 40 Hz responses. The value of the first bin is greater than 1 because of the short-term enhancement apparent during the first several responses. The *top gray dashed line* matches the steady-state response size for the last 21 responses when recorded at 20 Hz; the *bottom line* is drawn at exactly half that. Note that during the 40 Hz stimulation, the synaptic strength quickly settled to half that recorded at 20 Hz, matching the *bottom dashed line* and indicating that the RRP is left exhausted by the first 60 action potentials. *Inset*, The averages of the first 10 individual responses at 20 Hz, responses numbered 51–60 at 20 Hz, and the first 10 responses at 40 Hz are all scaled by their peak size and overlaid. Because the individual responses evoked at 40 Hz do not decay away completely in the 25 msec interstimulus interval, the corresponding tail of the average 20 Hz response was first scaled to match the prestimulus artifact baseline and then subtracted from the average 40 Hz response. Note that the shape of the EPSC did not change during the experiment. *B*, The stimulus intensity was set within the narrow threshold window as described in Results, and antidromic action potentials were recorded in CA3 pyramidal neurons as Schaffer collaterals were stimulated repetitively for 3 sec at 20 Hz and then for 1 sec at 40 Hz. The average probability of action potential firing given a stimulus (47 experiments, 2 neurons) was calculated for each second of stimulation and plotted versus time. Note that the firing probability did not change when the stimulus frequency was doubled (compare *bars 3 and 4*).

For example, it is possible that 20 Hz might represent an upper limit on the rate of action potential firing, in which case, increasing the stimulation frequency to 40 Hz would not increase the overall spike-firing rate in individual Schaffer collaterals. To control for this possibility, antidromic action potentials were recorded in the cell bodies of CA3 pyramidal neurons during a frequency-switching stimulation protocol similar to the one used above. Using this approach, the stimulating apparatus was found to have no problem evoking action potentials up to rates of at least 40 Hz.

To test rigorously whether changing the stimulus frequency had an effect on the excitability of Schaffer collaterals, we examined the firing behavior of axons when they were stimulated with the minimum strength that was required to evoke action potentials. By carefully adjusting the stimulation strength, we found a narrow range of settings in which a fraction of the stimuli would fail to trigger a regenerative current. This threshold window allowed the quantification of very small changes in axonal excitability over

the course of the experiment [Allen and Stevens (1994) and references therein].

Figure 1*B* shows that the average probability of firing did not change substantially during the experiment. Analysis was limited to trials during which some, but not all, of the individual stimuli during the first second of stimulation failed to elicit action potentials. No change was detected in the effective excitability of the Schaffer collaterals when the stimulation frequency was switched from 20 to 40 Hz (Fig. 1*B*, compare *bar 3 vs bar 4*). This experiment confirms that the stimulating apparatus was effective at evoking action potentials in the Schaffer collaterals at the frequencies used for this study. Taken together, these results indicate that doubling the frequency of presynaptic action potential firing did not substantially increase the rate of exocytosis in these experiments, confirming that a 20 Hz train of 60 action potentials is sufficient to nearly completely exhaust the RRP of these synapses.

### Residual steady-state RRP fullness

How close to empty is the pool after 3 sec of 20 Hz stimulation? The RRP is never expected to be truly empty for long periods because the replenishment process continuously supplies fresh quanta of transmitter to replace the spent ones. The average level of the remaining steady-state fraction depends on both the pool replenishment rate and the rate at which vesicles undergo exocytosis once they become available. Below, we introduce a formal model of pool replenishment that is used in the Appendix to show that doubling the stimulation frequency should lower the standing steady-state fullness of the RRP by a factor of  $\sim 2$ . As detailed in the Appendix, the steady-state levels of fullness at both stimulation frequencies can be estimated from the small, transient increase in the transmitter release rate that occurs as the sizes of the individual responses settle to a new steady state after the stimulus frequency is doubled. For the experiments documented in Figure 1*A*, the brief release rate increase was quantified from the small difference in the sum of the responses elicited by 40 Hz stimulation compared with the corresponding sum of responses during 20 Hz stimulation. The extra amount of release elicited by the 40 Hz stimulation was  $<2\%$  of the aggregate response elicited by the first 60 stimuli. We show in the Appendix how this predicts that the RRP of these Schaffer collateral synapses were  $<5\%$  full after 60 stimulations at 20 Hz.

### The RRP replenishment rate is slow at active synapses

The preliminary studies confirmed that our experimental preparation was appropriate for measuring the replenishment rate of the RRP at active synapses by showing that trains of at least 60 stimuli (20 Hz) are sufficient to drive the RRP into a near-empty steady state. Because synaptic vesicles can undergo exocytosis only after having been readied for release, the rate at which fresh transmitter becomes available defines the sustained rate of release when the RRP is in such a state. Likewise, the overall rate of transmitter release must be equivalent to the rate of RRP replenishment so long as stimulation is rapid enough to keep the pool in the near-empty steady state. An estimate of the rate constant for RRP replenishment can be determined by dividing this sustained rate of release from exhausted terminals by the total capacity of their RRP.

#### Lower bound for replenishment rate

The sum of all the responses evoked by the first 60 action potentials in a 20 Hz train yields an overestimate of the RRP

capacity. Because such a stimulus train leaves the RRP nearly empty, the sum of the responses must reflect release of the entire content of the pool, an amount that is equivalent to the RRP capacity if stimulation is initiated when the RRP is full. The replenishment process is continuous, however, so some fraction of the cumulative response reflects release of transmitter that became available during the 3 sec of stimulation.

The average response size during subsequent 20 Hz stimulation is directly proportional to the amount of pool replenishment that occurs during the brief interstimulus intervals, because each action potential leaves the RRP just as depleted as the previous one. Dividing the average response size during the fourth second of 20 Hz stimulation by the sum of the response sizes elicited by the first 60 action potentials yields a value of 0.75% for the data plotted in Figure 2*A* (14 slices). Because there are 20 action potentials per second, this translates into a standard rate constant of 0.15/sec. This would be the value of the RRP replenishment rate constant if no replenishment occurred during the first 3 sec of stimulation, and the sum of the first 60 responses was thereby directly proportional to the pool capacity. However, because the sum of the responses during the first 3 sec of stimulation is an overestimate of the true RRP capacity, 0.15/sec represents a lower bound for the RRP replenishment rate constant at active Schaffer collateral synapses.

#### Upper bound for replenishment rate

An upper bound can be calculated by assuming that the amount of RRP replenishment during each of the first 3 sec of stimulation is the same as it is during the fourth second when the refreshment rate can be estimated as the rate of exocytosis. If so, the release of freshly prepared transmitter would account for ~45% of the sum of responses elicited during the first 3 sec of stimulation. Excluding this fraction yields a rate constant for RRP replenishment of 0.28/sec. The release of replacement neurotransmitter is responsible for <45% of the cumulative quantity released, however, because the amount of replenishment during the first 2 sec of stimulation when the RRP is still partially full must be less than the corresponding quantity when almost all the release sites are vacant. The actual rate constant describing RRP replenishment therefore must fall somewhere between the lower 0.15/sec estimate and 0.28/sec.

We note that this upper bound is based on the generally accepted classic concept that a functionally definable RRP does indeed exist (Elmqvist and Quastel, 1965) and that the short-term depression observed during the first several seconds of heavy use is not caused instead by a progressive reduction in the ability of presynaptic terminals to mobilize other internal transmitter stores. It is likely that this is a valid principle because most of the alternative possibilities can be ruled out on the basis of data published previously elsewhere (Rosenmund and Stevens, 1996; Dobrunz and Stevens, 1997; Stevens and Wesseling, 1999a). Below, we provide an additional set of experiments designed to test even more thoroughly the integrity of the RRP itself.

#### A simple kinetic model for RRP replenishment

First, and to pinpoint the RRP replenishment rate constant within the range determined above, we present a quantitative model that allows us to gauge how much of the cumulative synaptic response was caused by the release of transmitter that became available during the experiments described above. Our simple model is depicted schematically in Figure 2*B* and is represented formally by Equation 1:

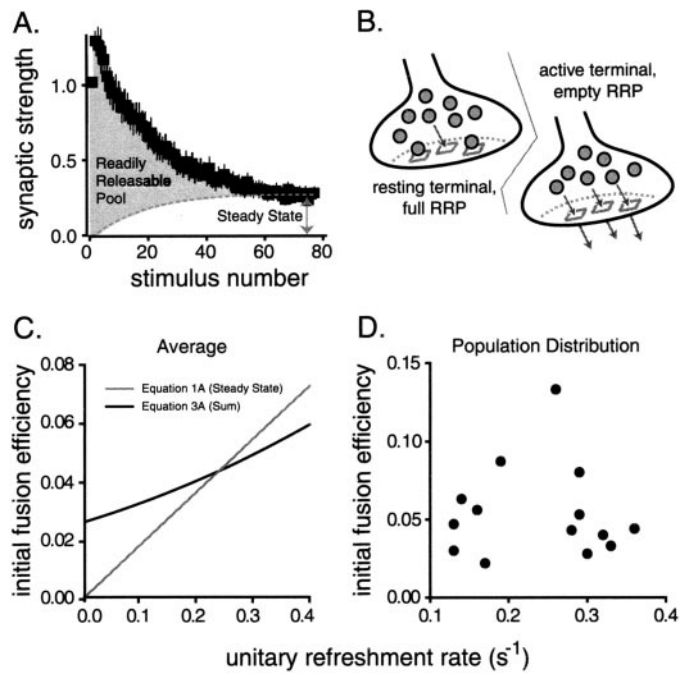


**Figure 2.** Readily releasable vesicles are replaced slowly during 20 Hz stimulation. *A*, Average relative synaptic strength is plotted as the Schaffer collateral synapses are stimulated at 20 Hz for 4 sec (each response was normalized by the size of the response to the first stimulus; experiments are from 14 slices). The dashed gray line represents the fraction of the synaptic response that is predicted to result from the exocytosis of vesicles that became available for release during the experiment (as derived in the Appendix). *B*, Working model of RRP replenishment. *Left panel*, In the resting synapse the spontaneous rate of exocytosis is low, and the RRP fills completely. The pool has a maximum capacity, and the high-energy barrier that keeps vesicles from fusing spontaneously is the rate-limiting element that controls how quickly synaptic vesicles undergo exocytosis. *Right panel*, Episodes of high-frequency activity drive exocytosis quickly enough to exhaust the RRP. With the pool empty, the rate at which new vesicles are made available limits the rate of transmitter release; the energy barrier to fusion prevents vesicles from undergoing exocytosis in the interval between action potentials, but as long as the high-frequency spike train continues, the barrier is no longer the rate-limiting element in the exocytic/endocytic cycle. This model accounts only for rate-limiting steps in the exocytic/endocytic cycle during the first several seconds of heavy use. Thereafter an additional element plays a role in controlling the dynamics of neurotransmitter mobilization. Endocytosis does not play a rate-limiting role in this scheme and is not represented here. *C*, The simultaneous solutions for Equations 1A and 3A (Appendix) are plotted for the data shown in *A*. The two independent equations relate the rate constant of pool replenishment to the fraction of the full pool triggered to release by isolated action potentials (fusion efficiency). When the corresponding values for the two parameters are plotted against each other, the resulting lines intersect where the refilling rate constant equals 0.24/sec and the initial fusion efficiency is 0.044. Equation 1A depends only on the steady-state response size after the pool has reached a near-empty steady state and is represented by the gray diagonal line. Equation 3A depends on the changing rate at which transmitter was released over the complete course of the experiment and is represented by the black line. *D*, The initial fusion efficiency and the pool replenishment rate constant were estimated separately by simultaneously solving Equations 1A and 3A for each of the 14 experiments summarized in *A* and plotted versus each other. Note that there is no evident correlation between these two parameters.

$$\frac{dn}{dt} = \alpha \cdot (N - n) - \beta \cdot n, \quad (1)$$

where the rate constant of pool filling,  $\alpha$ , is the parameter that we evaluate,  $\beta$  is the unitary rate of exocytosis,  $n$  represents the

number of vesicles available for release, and  $N$  is the capacity of the RRP (i.e., the total number of release sites in the RRP).

Equation 1 describes a realistic general model of RRP dynamics during the first several seconds of high-frequency use. It assumes a pool of a fixed size ( $N$ ) containing individual sites that fill independently with first-order kinetics. The differential equation is equivalent to the one used to characterize the kinetics of pool replenishment in one of the earliest papers describing the time course of RRP refilling at central synapses (Stevens and Tsujimoto, 1995). Several nontrivial predictions of the model have since been tested, and it remains the simplest scheme that is consistent with what is known about the kinetics of RRP replenishment. For example, the rate at which vesicles leave the RRP without undergoing exocytosis has been shown to be slow compared with the rate of pool filling (Murthy and Stevens, 1999). This, along with other observations (Stevens and Wesseling, 1998, 1999b; Pyott and Rosenmund, 2002), implies that the pool has a fixed size and is not instead in some steady-state equilibrium with a larger reserve pool (the reverse reaction would formally be a negligible component of  $\beta$ ). An additional rate-limiting element in the synaptic vesicle exocytic/endocytic cycle plays a role during more extensive use (Stevens and Wesseling, 1999b).

Equation 1 provides enough constraints to calculate the replenishment rate constant ( $\alpha$ ) from the data plotted in Figure 2*A*, as outlined in the Appendix. The fraction of the total response generated by transmitter that became available for release after stimulation was initiated is plotted as a *dashed line* in Figure 2*A*. The simultaneous solution of two independent equations derived from Equation 1 (Eqs. 1*A* and 3*A*) yields an average value for  $\alpha$  of 0.24/sec for the experiments summarized in Figure 2*A* ( $n = 14$  slices). Although it is possible to devise alternative models that generate slightly different estimates, the actual refreshment rate could not be much faster, because this estimate is close to the upper bound (0.28/sec) derived without the constraints of a specific model. It thus typically takes several seconds for fresh packets of neurotransmitter to replace the expended readily releasable supply during episodes of intense synaptic use.

### Estimates of fusion efficiency

Equation 1 also provides information about the efficiency with which action potentials trigger exocytosis that can be used as a consistency check for the logic presented so far. Although the present analysis does not provide meaningful absolute units for  $N$  because neither the number of synapses activated simultaneously nor the quantal response sizes are known, the fraction of the RRP that was triggered to undergo exocytosis by the first action potential in each 20 Hz train can be calculated by dividing the size of the first response by  $N$ . This fraction is termed the initial fusion efficiency because it represents the efficiency with which isolated action potentials trigger the release of available vesicles at resting synapses (Stevens and Wesseling, 1999a). The common solution for Equations 1*A* and 3*A* yields a value for this parameter of 0.044, for the experiments summarized in Figure 2. (The individual solutions for the two equations for the data plotted in Fig. 2*A* are plotted in Fig. 2*C*.) This value fits within the published range of 0.03–0.07 for these synapses, giving us confidence that our approach measures the same kinetic elements that have been studied previously (Dobrunz and Stevens, 1997; Schikorski and Stevens, 1997). Although we did observe a significant amount of heterogeneity between preparations in both the rate of RRP replenishment [range, 0.13–0.36; coefficient of variation (CV) = 0.33; see also Stevens and Wesseling (1998)] and the initial fusion

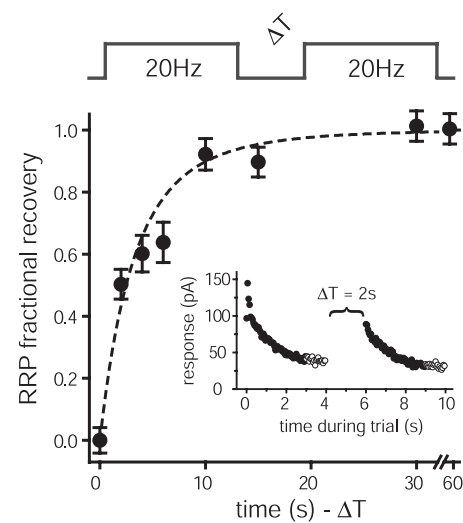


**Figure 3.** The RRP replenishment time course during periods of rest is predicted by the refreshment rate when synapses are active. The RRP was emptied with 80 action potentials (20 Hz), and subsequent recovery was monitored after an experimentally varied delay with an identical burst of stimulation (diagrammed at *top*). The sums of the responses to the second stimulus train were normalized as described in Results and plotted against the recovery interval. The curve is the predicted RRP refilling time course calculated with Equation 2 from the replenishment rate measured when the synapses were active (0.30/sec for these synapses; mean  $\pm$  SEM; 9 cells, at least 10 trials for each point). *Inset*, Average synaptic strengths of the responses elicited during the first and second stimulus trains for the 2 sec recovery interval are plotted versus time during the trial (*filled circles* represent the responses that were used to estimate the RRP recovery after 2 sec of rest, i.e., the first 60 responses of each stimulus train).

efficiency (range 0.022–0.13; CV = 0.52), Figure 2*D* shows that the variation was not correlated between the two parameters ( $r = 0.01$ ).

### Slowly dissipating, activity-dependent acceleration of the replenishment process

Is neurotransmitter prepared for exocytosis much more quickly at active nerve terminals than at quiescent ones? The average replenishment rate constant of 0.24/sec that we have determined for the RRP of active Schaffer collateral synapses is not much faster, if at all, than the resting refreshment rate measured at similar types of synapses grown in cell culture [which range from 0.09/sec to 0.4/sec (Stevens and Wesseling, 1998)]. To compare the replenishment rate during high-frequency stimulation with the rate during rest intervals at the same Schaffer collateral synapses, we measured the complete time course over which the RRP refills after being depleted.

The experimental strategy used is conceptually similar to previously published methods (Stevens and Tsujimoto, 1995; Stevens and Wesseling, 1999b). Experiments were conducted during which the pool was emptied two times in succession, with an experimentally varied rest interval as diagrammed at the top of Figure 3. Trains of action potentials (80 at 20 Hz) were used instead of osmotic shocks to elicit exocytosis from the synaptic terminals. An estimate of pool refilling during the rest interval was derived by dividing the sum of the first 60 responses during the second stimulus train by the corresponding sum of responses evoked by the first one. To account for the steady-state amount of release that persists after the RRP has already been exhausted, the sums were first adjusted by subtracting the equivalent measure

derived from experiments when no time was allowed for recovery between the two stimulus trains.

As anticipated from Stevens and Wesseling (1998), the replenishment rate at Schaffer collateral synapses during long recovery periods is somewhat slower than the value for  $\alpha$  estimated when the synapses are active. If the replenishment process remained constant after stimulation ceased, Equation 1 would predict a single exponential time course of refilling with a time constant of 3.3 sec (i.e.,  $1/\alpha$ ,  $\alpha = 0.30/\text{sec}$  for this particular set of synapses). Instead, however, the recovery time course was more closely approximated by a somewhat slower, 5 sec exponential (recovery data are plotted in Fig. 3; the single exponential is not shown). This difference was expected because the residual calcium that accumulates in presynaptic terminals during high-frequency use has been shown to accelerate the replenishment process several-fold (Stevens and Wesseling, 1998). During subsequent periods of rest, the rate diminishes gradually as residual calcium is pumped out of the terminals. Equation 1 can be modified to account for the decaying effect of residual calcium during rest intervals, yielding:

$$n(t) = N \cdot (1 - e^{-\int \alpha(t) dt}), \quad (2)$$

where  $\alpha(t)$  is no longer a constant but decays to baseline along a single exponential with a time constant of 10 sec during periods of rest (Stevens and Wesseling, 1998). If  $\alpha(t)$  starts at 0.30/sec at the beginning of the recovery period and then slows down threefold, Equation 2 yields the *dashed line* in Figure 3, which provides a good approximation for the recovery time course.

The estimate of the RRP replenishment rate at active synapses is thus consistent with the measured time course of pool refilling during subsequent periods of rest. The slowly decaying, residual calcium-dependent acceleration appears to be the only significant kinetic element that increases the rate at which neurotransmitter becomes available for release during periods of heavy use.

### Pool capacity does not depend on the measurement methodology

Although the conclusion that it takes several seconds for fresh vesicles laden with neurotransmitter to be prepared for exocytosis at active synapses does not depend on the particular formal theory used to calculate the RRP refreshment rate, it is based on the classic concept that a functionally definable subset of the synaptic vesicles is available for action potential-triggered exocytosis. To test this generally accepted assumption more thoroughly, we investigated the effects of changing either the efficiency with which individual action potentials trigger the exocytosis of readily releasable vesicles, or the rate of stimulation, on our measure of pool capacity.

#### Calcium

Raising the extracellular concentration of calcium enhances the strength of resting synapses by increasing the efficiency with which action potentials trigger exocytosis of release-ready vesicles, whereas magnesium has the opposite effect [Stevens and Wesseling (1999a) and references therein]. Changing the ratio of the two divalent ions should not affect measurements of RRP capacity if the RRP is a pool of fixed size.

The capacity of the pool was measured from the responses to 80 stimuli (20 Hz), with either 4.5 mM Ca/0.5 mM Mg or 2.5 mM Ca/2.5 mM Mg in the bath; the normalized response sizes are plotted in Figure 4*Ai*. The total divalent ion concentration was kept constant because axonal excitability can be influenced by this param-

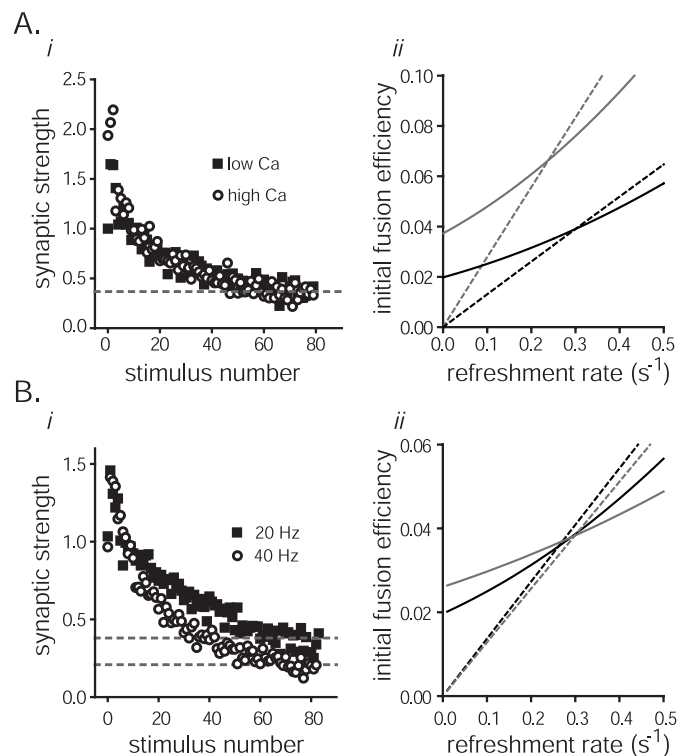


**Figure 4.** The capacity of the RRP does not depend on the measurement protocol. *A*, Short-term depression was induced with 80 stimuli (20 Hz) with either 2.5 mM Ca/2.5 mM Mg (*squares*) in the bath or 4.5 Ca/0.5 Mg (*circles*) at the same synapses. *i*, Responses were normalized by the average size of the first response recorded at the lower calcium concentration and plotted versus stimulus number (3 slices, 7 trials for each). *ii*, The RRP replenishment rate constant and the initial fusion efficiency were calculated by simultaneously solving Equations 1A and 3A, as in Figure 2C. The *gray lines* represent the analysis of responses evoked under the high calcium condition; the *black lines* are for the lower calcium experiments. The *dashed lines* represent the solutions for Equation 1A; the *solid lines* represent Equation 3A. Points of intersection represent the common solutions. Note that, as predicted, the fusion efficiency in high calcium is greater than the fusion efficiency in low calcium by a factor similar to the amount of enhancement in synaptic strength observed after switching into the higher calcium-containing solution. *B*, Depression was induced with 81 stimuli at 20 and 40 Hz for the same synapses. *i*, The response sizes were normalized by the average size of the first responses in the stimulus trains and plotted versus stimulus number for both sets of trials (3 slices, 11 trials for each). *ii*, Simultaneous solution of Equations 1A (*dashed lines*) and 3A (*solid lines*). The *gray lines* represent the analysis of the 40 Hz responses; *black lines* represent the analysis of 20 Hz responses.

eter (Franks-Haeuser and Hodgkin, 1957). At the higher calcium concentration, the average size of the first synaptic response during stimulation was approximately twice the size of the corresponding one measured with the lower calcium concentration in the bath. The synaptic strength depressed so much more quickly in higher calcium, however, that the sums of all 80 responses were statistically indistinguishable between the two conditions.

Neither the RRP capacity nor the replenishment rate calculated as outlined in the Appendix differed significantly between conditions. The measured capacity was slightly larger under the high calcium condition (9%), and the replenishment rate was slightly lower (0.26 vs 0.31/sec), both differences reflecting a nonsignificantly lower (5%) average steady-state response to the final 20 stimuli under the high calcium condition. As expected, the increase in the initial fusion efficiency calculated from the simul-

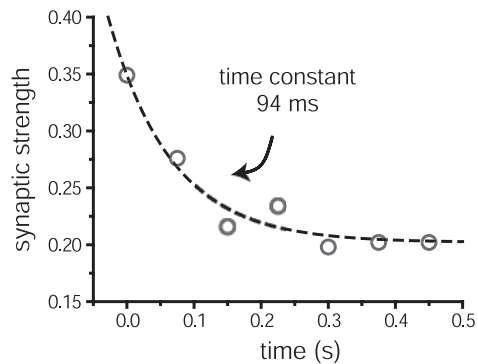


**Figure 5.** The working model predicts the synaptic response settling time course when the stimulation frequency is doubled after the RRP has been emptied. The circles represent the relative synaptic strength during the 40 Hz stimulation (also plotted on a smaller scale as open circles in Fig. 1*A*). The dashed line is the prediction generated by Equation 1 in the Appendix and depends on the integral of the small transient increase in the overall rate of exocytosis that occurs after switching frequencies from 20 to 40 Hz.

taneous solutions of Equations 1*A* and 3*A* for both sets of data (Fig. 4*Aii*) closely matched the increase in synaptic strength that occurred when the calcium to magnesium ratio was increased.

#### Stimulation frequency

The measurement of RRP capacity should also be independent of the particular stimulation protocol used to empty it. To test this, pool capacity was measured from 80 responses generated at either 20 or 40 Hz (Fig. 4*B*). Although the sum of the responses evoked by the first 60 stimuli at 20 Hz was 28% greater than the corresponding sum of responses to 60 action potentials recorded at 40 Hz, this difference was expected because there was twice as much time for replacement transmitter to become available for release during the slower stimulus trains. When this factor is taken into account as outlined in the Appendix, the resting capacity estimated from the responses evoked by the 20 Hz stimulation was within 5% of the value derived from the 40 Hz trials. The solutions of Equations 1*A* and 3*A* are plotted in Figure 4*Bii*. As expected, the RRP replenishment rate constants were similar for the two data sets (0.29/sec for the 40 Hz stimulation protocol and 0.26/sec for the 20 Hz protocol).

Together, these results indicate that the capacity of the RRP does not depend on the particular protocol used to measure it. They provide support for the general concept that the neurotransmitter used for synaptic signaling is drawn from a nonarbitrary RRP (Birks and MacIntosh, 1961; Elmqvist and Quastel, 1965) and for our particular model of RRP replenishment (Eq. 1).

#### A test of Equation 1 in particular

Further analysis of the experiments already summarized in Figure 1*A* provides another, independent test of our specific model. In addition to predicting the average fullness of the RRP under near-empty steady-state conditions, Equation 1 provides enough constraints to predict quantitatively the time course of transition over which a new steady state is achieved when the frequency of stimulation is suddenly doubled, as it was in those experiments. The predicted time course follows a single exponential with a time constant of 94 msec (as derived in the Appendix). Figure 5 shows that this prediction corresponds well with the observed time course of decay in synaptic strength.

#### Controls indicating that postsynaptic responses linearly track exocytic rates

As mentioned above, the analysis presented in this report relies on the assumption that postsynaptic responses can be used as linear detectors of the amount of transmitter release at these synapses during 20 and 40 Hz use. This would not be a valid assumption for some other types of central synapses in which postsynaptic elements of short-term plasticity have been observed. Following are a series of controls designed to confirm the conclusions of earlier reports (Dobrunz and Stevens, 1997) indicating that postsynaptic receptors faithfully track transmitter release at the Schaffer collateral synapses used in this study.

#### Receptor desensitization

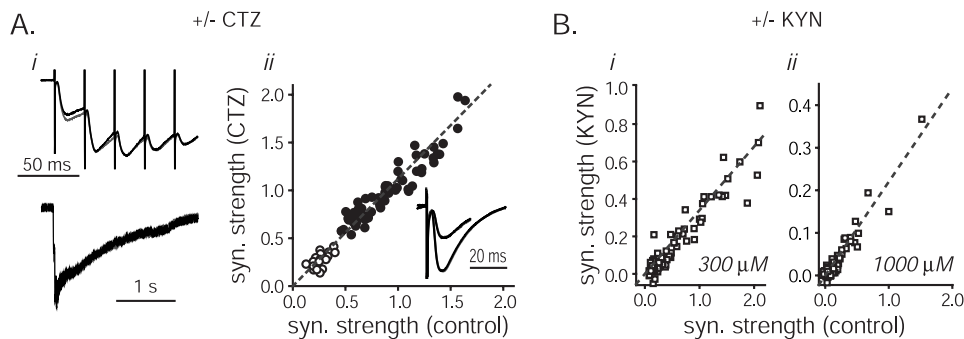
At some types of synapses, postsynaptic receptor desensitization contributes to short-term depression (Trussell et al., 1993). To confirm that receptor desensitization did not contribute to the rapid decrease in synaptic strength that occurred during stimulation frequencies of 20 and 40 Hz, or when the stimulating frequency was increased during stimulation, experiments similar to those documented in Figures 1*A* and 4*B* were conducted in the presence and absence of 100  $\mu$ M CTZ, a drug that blocks glutamate receptor desensitization (Patneau et al., 1993; Yamada and Tang, 1993).

Figure 6*A* shows that receptor desensitization does not play a role in the short-term depression observed in these experiments. CTZ did cause a 12% increase in the amplitudes of the synaptic responses, an effect that may be attributable to alleviation of receptor desensitization that ordinarily partially shapes individual postsynaptic responses or to some other effect of CTZ on glutamate receptor kinetics (Yamada and Tang, 1993). However, the relative increase was the same for all responses elicited by the stimulus trains, as reflected in the slope of 1.12 for the straight line in Figure 6*Aii*. Postsynaptic receptor desensitization thus played no apparent role in short-term depression even at stimulation rates as high as 40 Hz.

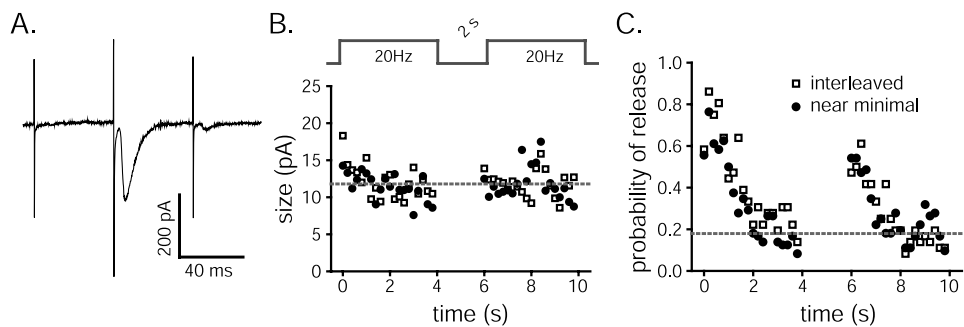
#### Receptor saturation and voltage-clamp errors

The glutamate receptor antagonist KYN was used in an additional control designed to test for other unanticipated nonlinearities in the postsynaptic response to the release of neurotransmitter at 40 Hz. For example, it has been suggested that the glutamate released from a single vesicle may bind to between 70 and 90% of all receptor binding sites, saturating the response at individual synapses (Jonas et al., 1993; Diamond and Jahr, 1997) (but see Liu et al., 1999; McAllister and Stevens, 2000). If multiple vesicles are released simultaneously more often at individual synapses when the probability of release is high, this phenomenon might have affected the linearity of our postsynaptic measurements and caused us to underestimate the true amount of depression in the release of transmitter from the presynaptic terminals (for review, see Auger and Marty, 2000). A large space/voltage-clamp error in our patch-clamping technique could have had a similarly misleading effect.

Synaptic responses to 80 stimuli (40 Hz) were recorded in the presence and absence of 300 and 1000  $\mu$ M KYN in separate sets of experiments. KYN competitively blocks glutamate binding to the non-NMDA ionotropic receptors used to track transmitter release in this study. This drug dissociates rapidly enough on the time scale of transmitter clearance from the synaptic cleft that it lowers the effective affinity of the glutamate receptors for glutamate (Diamond and Jahr, 1997). The same quantitative models



are plotted in the *bottom panel*. *Aii*, Twenty Hertz and frequency switching. Schaffer collaterals were stimulated 60 times at 20 Hz and then 21 more times at 40 Hz as in Figure 1*A* in the presence and absence of 100  $\mu\text{M}$  CTZ. The size of the synaptic response to each stimulus was normalized by the average size of the first control response (no drug). The size of each response recorded in CTZ is plotted against the size of the corresponding control response to the same stimulus number (*open circles* represent responses at 40 Hz; *filled circles* are 20 Hz responses). The *dashed gray line* is straight, with a slope of 1.12 (3 slices, 10 trials each). *Inset*, The average current traces representing the responses to the 20 stimuli preceding and after the frequency switch for each condition are overlaid (the response recorded in the absence of drug was scaled by 1.12; the larger of the two sets of current deflections represents responses recorded at 20 Hz; the baseline of the 40 Hz response average was calculated and subtracted as for the *inset* of Fig. 1*A*). Note that the scaled responses with and without drug are identical and that the average 40 Hz response size is approximately half that recorded at 20 Hz. *B*, Schaffer collaterals were stimulated at least 80 times at 40 Hz alternately in the presence and absence of KYN (300  $\mu\text{M}$ : 3 slices, 22 trials each; 1000  $\mu\text{M}$ : 3 slices, 10 trials each). The normalized sizes of the control responses are plotted against the corresponding sizes of the responses gathered with KYN in the bath for each stimulus (*i*, 300  $\mu\text{M}$  KYN; *ii*, 1000  $\mu\text{M}$  KYN). The *dashed lines* are straight with slopes of 0.34 (*i*) and 0.22 (*ii*).



eraged into 200 msec bins and plotted versus the time of the experiment. The *squares* represent the interleaved minimal responses; the *circles* summarize experiments in which only minimal stimuli were used throughout.

that predict glutamate receptor saturation during normal synaptic transmission also predict that, in addition to partially blocking the synaptic response,  $\geq 300 \mu\text{M}$  KYN should shift the dose–response relationship between transmitter release and postsynaptic response size well into the linear range (Diamond and Jahr, 1997). Figure 6*B* shows that neither treatment affected the accumulation of short-term depression, however, indicating that receptor saturation does not introduce a nonlinear component into our postsynaptic measure of transmitter release. Furthermore, KYN did reduce the overall synaptic strength substantially (66% in 300  $\mu\text{M}$  KYN, 78% in 1000  $\mu\text{M}$  KYN), making it unlikely that voltage-clamp errors contributed significant nonlinearities to our measurements.

#### Intersynaptic cross talk

Finally, we provide a positive control for our assumption that the postsynaptic responses to Schaffer collateral stimulation can be used as linear estimators of transmitter release. The CTZ and KYN experiments argue against receptor desensitization or saturation as significant contributions to short-term plasticity, but do not necessarily address other potential postsynaptic mechanisms. A more direct test has been provided by Dobrunz and Stevens (1997), who showed that the quantal sizes of responses to transmitter released from single synapses do not depress during repetitive use, when stimulus strengths are so weak that only one

Figure 6. CTZ and KYN do not affect short-term depression. *Ai*, Forty Hertz stimulation. Schaffer collaterals were stimulated 80 times at 40 Hz in the presence and absence of 100  $\mu\text{M}$  CTZ. Average responses to the stimulus trains with (gray traces) and without (black traces; scaled by 1.12) CTZ are plotted (data are from 4 slices, 18 trials for each). The first six responses are plotted in the *top panel*. Note that CTZ amplified the first response slightly more than the rest, possibly because of presynaptic side effects of the drug. The entire electrophysiological recordings (the trace gathered in the absence of drug is scaled by 1.12), with the stimulus artifacts blanked (2 msec windows),

are plotted in the *bottom panel*. *Aii*, Twenty Hertz and frequency switching. Schaffer collaterals were stimulated 60 times at 20 Hz and then 21 more times at 40 Hz as in Figure 1*A* in the presence and absence of 100  $\mu\text{M}$  CTZ. The size of the synaptic response to each stimulus was normalized by the average size of the first control response (no drug). The size of each response recorded in CTZ is plotted against the size of the corresponding control response to the same stimulus number (*open circles* represent responses at 40 Hz; *filled circles* are 20 Hz responses). The *dashed gray line* is straight, with a slope of 1.12 (3 slices, 10 trials each). *Inset*, The average current traces representing the responses to the 20 stimuli preceding and after the frequency switch for each condition are overlaid (the response recorded in the absence of drug was scaled by 1.12; the larger of the two sets of current deflections represents responses recorded at 20 Hz; the baseline of the 40 Hz response average was calculated and subtracted as for the *inset* of Fig. 1*A*). Note that the scaled responses with and without drug are identical and that the average 40 Hz response size is approximately half that recorded at 20 Hz. *B*, Schaffer collaterals were stimulated at least 80 times at 40 Hz alternately in the presence and absence of KYN (300  $\mu\text{M}$ : 3 slices, 22 trials each; 1000  $\mu\text{M}$ : 3 slices, 10 trials each). The normalized sizes of the control responses are plotted against the corresponding sizes of the responses gathered with KYN in the bath for each stimulus (*i*, 300  $\mu\text{M}$  KYN; *ii*, 1000  $\mu\text{M}$  KYN). The *dashed lines* are straight with slopes of 0.34 (*i*) and 0.22 (*ii*).

Figure 7. Individual synapses behave like simultaneously activated populations. Schaffer collaterals were stimulated with pairs of 4-sec-long spike trains (20 Hz) separated by 2 sec intervals. For half of the trials, only a minimal number of afferents were stimulated throughout. For the other half, stimuli of normal intensity were interleaved with the weak stimuli. *A*, Typical, sequential raw data example of a failure, a large response, and a minimal response during interleaved stimulation. *B*, *C*, The average sizes (*B*) and probability (*C*) of successful transmissions in response to the minimal stimuli were averaged

afferent synapse is activated at once. We typically evoked release from tens of synapses simultaneously for our experiments, however. Although there is no indication that transmitter released at the same time from multiple synapses interacts with the AMPA type of glutamate receptors in a nonlinear way at Schaffer collateral synapses (Asztely et al., 1997), cross talk between calyceal-type synapses has been reported to result in postsynaptic forms of short-term depression (Trussell et al., 1993; Neher and Sakaba, 2001). Such a phenomenon, if operative at Schaffer collateral synapses, might have led to an overestimate of the actual amount of presynaptic depression in our experiments.

An experiment designed to test this possibility instead verified that the amount of depression in synaptic strength measured at multiple, simultaneously active synapses was matched by decreases in the probability of release at individual synapses. Short-term depression and RRP refilling were measured with pairs of stimulus trains (80 stimuli at 20 Hz) separated by 2 sec rest intervals as diagrammed at the top of Figure 7*B*. Weak stimuli were interleaved with those of normal strength during experimental trials. The weak stimulus intensities may have evoked action potentials in several axons, all with afferent synapses with low release probabilities, or in single afferent synapses. Experimental trials were alternated with control trials during which only weak



stimuli were used throughout. Cross talk between synapses would be measurable as a change in the sizes of the successful responses to weak stimulation caused by transmitter release elicited by the normal intensity stimuli.

Figure 7 shows that neither the size of the successful minimal responses (Fig. 7*B*) nor the probability of release (Fig. 7*C*) was affected by the transmitter release elicited by the large, interleaved stimuli. This result argues strongly against a contribution of intersynaptic cross talk to short-term depression.

The average amplitude of the successful minimal responses during both types of trials may have declined a small amount during the first second of stimulation (Fig. 7*B*). The effect is attributable to the infrequent, simultaneous exocytosis of multiple vesicles, as expected of a stochastic release process when the overall probability of release is as high as it was at the beginning of the weak stimuli trains (Zucker, 1973).

During 20 Hz use, the probability of release at the synapses activated by the weak stimuli depressed just as extensively as the synaptic currents did in the other experiments reported here. The RRP refreshment rate constant calculated by the method outlined in the Appendix for the data plotted in Figure 7*C* is 0.23/sec. This value is indistinguishable from the rate constant calculated from the synaptic currents elicited by stronger stimulations. The RRP refilled ~45% during the first 2 sec of rest, yielding an extrapolated replenishment rate constant of 0.30/sec, a value that is not significantly different from the rate constant calculated for the synapses when active. These results provide assurance that the synaptic currents measured for this study were linearly related to the amount of release at multiple, simultaneously active synapses, and they confirm that it takes several seconds for neurotransmitter to replenish the RRP, even when synapses are active.

## DISCUSSION

Here we show that a slowly dissipating, residual calcium-driven acceleration mechanism is sufficient to account for the full range of activity-dependent modulation of the rate at which neurotransmitter is prepared for exocytosis at Schaffer collateral synapses. Fresh quanta of neurotransmitter were found to replace spent ones in the RRP at an average rate of 0.24/sec when synapses were active. During subsequent periods of rest, the RRP refilled with an ~5 sec exponential time course, as expected if the replenishment process were to gradually decelerate during inactive periods as demonstrated previously (Stevens and Wesseling, 1998). With no deceleration during rest intervals, the 0.24/sec rate constant would predict an only slightly faster exponential refilling time course with a 4.2 sec time constant. This leaves little kinetic room for a rapidly dissipating component of replenishment-rate enhancement that might have been missed by the earlier study and indicates that the rate at which the RRP is replenished can be accelerated only modestly, even during periods of heavy synaptic use.

A kinetically simple model (Eq. 1) of the rate-limiting mechanisms that control how long it takes for neurotransmitter to be prepared for release provides a good account of the dynamics of short-term plasticity analyzed here. In particular, Figure 5 shows that when the RRP is in a near-empty steady state, our working model predicts quantitatively the time course over which the synaptic strength settles to a new steady state after perturbations in the stimulus frequency, a behavior that is a hallmark of first-order kinetic reactions.

Although the cell biological process of vesicular maturation is complex, involving endocytosis, vesicle genesis and loading, phys-

ical translocation and docking to the release sites, and biochemical priming (Sudhof, 1995), the observation that first-order kinetics describe well the process by which vesicles are readied for exocytosis is consistent with the possibility that only a single first-order enzymatic step in the exocytic/endocytic cycle is rate limiting during the first several seconds of heavy synaptic use. The identity of the molecular machinery that limits how quickly vesicles are prepared for exocytosis remains obscure, although it seems to be enzymatic in nature (Stevens and Wesseling, 1998, 1999b; Pyott and Rosenmund, 2002) and may be related to biochemical priming that takes place during or after physical docking to the active zone (Kawasaki et al., 1998). During extended periods of synaptic activity, a second rate-limiting process also plays a role in a longer-lasting form of synaptic depression that may be related to depletion of the reserve pool of vesicles or to some other rate-limiting element in the exocytic/endocytic cycle (Stevens and Wesseling, 1999b).

### Does the readily releasable pool have kinetic subdivisions?

Our working model makes no qualitative kinetic distinctions among readily releasable vesicles. The data presented here are also consistent with models in which some of the release-ready vesicles are available for immediate exocytosis, and the rest are used to restock quickly this smaller pool when required, as long as the rate of transfer between the two pools is fast on the time scale of these experiments (Neher and Zucker, 1993; Voets et al., 1999; Voets, 2000). On the other hand, the phenomena modeled by these more complicated schemes can often be explained equally well if the efficiency with which action potentials trigger the fusion of individual release-ready vesicles is a heterogeneous property of the release sites themselves (Beutner et al., 2001; Sakaba and Neher, 2001). At present, we favor models in which all of the release-ready vesicles are prevented from undergoing exocytosis by a single type of energy barrier, because when the release process is enhanced by residual calcium, the propensity for exocytosis of the whole pool is potentiated in parallel (Stevens and Wesseling, 1999a).

### Relation to earlier studies

On the basis of electrophysiological data alone, the RRP refreshment rate that we have measured may pertain either to the time it takes for reserve vesicles to be prepared for release or to some other mechanism of neurotransmitter mobilization such as direct refilling of the depleted readily releasable vesicles themselves. However, Pyle et al. (2000) recently measured the time it takes for fluorescently labeled reserve vesicles to replace spent readily releasable ones during periods of rest after episodes of high-frequency synaptic use at similar synapses in culture. They report a single exponential recovery time course with a 7 sec time constant, derived from optical measurements, that is similar to the 5 sec time constant for RRP refilling measured here, suggesting that the RRP is replenished primarily with waiting reserve vesicles and not by some other means.

Several studies have reported that the transmitter mobilization process is much faster when synapses are active than it is during subsequent rest intervals (Kusano and Landau, 1975; Pyle et al., 2000). In the earliest study to report such a phenomenon, Kusano and Landau (1975) used a model in which action potentials always release the same fraction of the RRP, and they concluded that the amount of short-term depression observed during high-frequency use is incompatible with a slow replenishment process at the

squid giant synapse. It is now known, however, that the efficiency with which action potentials trigger release is not stationary at the mammalian central synapses that we study (Stevens and Wesseling, 1999a). Although squid synapses may behave differently from Schaffer collateral synapses in this respect, it is also possible that the short-term depression in synaptic strength measured by Kusano and Landau (1975) did not correspond to the true extent of RRP depletion, much as a similar analysis would lead to an underestimate of pool depletion for the synapses in our preparation. Such an underestimate may have led to an overestimate of the amount of activity-dependent acceleration in the replenishment process at the squid giant synapse.

Pyle et al. (2000) reported a faster time course for RRP refilling when measured electrophysiologically, from which they have concluded that individual readily releasable vesicles can be reused rapidly several times before being replaced at a slower rate by vesicles from the reserve pool. The basis of our quantitatively differing electrophysiological results is uncertain. One possibility is that the stimulation protocol used by Pyle et al. (2000) to elicit exocytosis in the electrophysiological portion of their study did not completely empty the available pool. This might have resulted in a recovery time course that partially reflected short-term enhancement in that a larger fraction of the available pool would have been released by trains initiated after shorter rest intervals than by those initiated after longer periods of rest [for a more extensive discussion of this issue, see Stevens and Wesseling (1999a)].

### What is the role of the RRP?

The release-ready supply of synaptic vesicles supports the ability of synapses to communicate information encoded by the spike-firing rate. The hippocampal synapses that we have studied start with a typical release probability of ~30–40% (Hessler et al., 1993; Rosenmund et al., 1993; Allen and Stevens, 1994; Huang and Stevens, 1997). Although they fail to release transmitter in response to most individual action potentials, they can still reliably transmit information by using short bursts of action potentials that are sure to trigger some exocytosis when the RRP is at least partially full. However, this option is no longer available to synapses that have expended all of their release ready vesicles. After the RRP has been exhausted, the probability of release becomes inversely proportional to the stimulus frequency (Eccles and Rall, 1951; Curtis and Eccles, 1960; Elmqvist and Quastel, 1965; Abbott et al., 1997). Because transmitter release is stochastic and rare when synapses are depleted of their release-ready vesicles, increasing the frequency of presynaptic activity would have minimal impact on the overall signal detected by postsynaptic neurons.

Because of the kinetic constraints imposed by a slow RRP replenishment rate, information would likely be transmitted more efficiently via these synapses by a neural code that relies on sporadic bursts of activity than on one that uses precise modulations in the frequency of continuous activity. Consistent with this, excitatory neurons in the hippocampus and other brain regions do tend to fire such bursts of spikes in awake and behaving mammals (Ranck, 1973; Scott et al., 1986; Newsome et al., 1989; Knierim and van Essen, 1992; Meister and Berry, 1999). This raises the following question: is the slow replenishment rate an unavoidable biochemical limitation that hampers the design of efficient neural circuits, or does the nervous system derive some computational benefit from such constraints on synaptic operation?

## APPENDIX

### Derivation of the RRP refreshment rate from Equation 1

According to Equation 1, when the RRP starts off empty, and there is no exocytosis (i.e.,  $\beta = 0$ ), the pool replenishes as a function of time by:

$$n(t) = N \cdot (1 - e^{-\alpha t}).$$

These conditions are approximated during the brief intervals between stimuli when the RRP is in a near-empty steady state, as it is after the 60th action potential in a high-frequency train. While the pool is maintained in a steady state, the amount of refilling between stimuli must be equivalent to the amount of exocytosis,  $r(\infty)$ , elicited by each action potential. If  $\nu$  is the frequency of stimulation (20 Hz or 40 Hz for this study):

$$r(\infty) = N \cdot (1 - e^{-\frac{\alpha}{\nu}}),$$

because  $1/\nu$  is the time between stimuli. The solution for  $\alpha$  depends on the pool capacity,  $N$ , which turns out to be an unwieldy parameter. A more convenient parameter is the initial fusion efficiency,  $fe$ , defined as the fraction of the RRP released by the first stimulus:

$$fe = \frac{r(1)}{N},$$

where  $r(1)$  is the amount of transmitter released by the first stimulus. By rearranging, and substituting for  $N$ :

$$fe = \frac{r(1)}{r(\infty)} \cdot (1 - e^{-\frac{\alpha}{\nu}}). \quad (1A)$$

This equation relates two unknown variables,  $fe$  and  $\alpha$ , and depends on the steady-state rate of release elicited during continued stimulation after the RRP has been emptied.

Another, independent equation relating the two unknown variables can be derived from Equation 1 that, in contrast, depends on the rate of transmitter release during the first part of a high-frequency train. The capacity of the pool (and thence the fusion efficiency) could be estimated crudely by summing all of the quanta released by the first 60 action potentials, but this method overestimates the true capacity because fresh vesicles that replace those expended during stimulation are also released. The true capacity is:

$$N = \sum_{i=1}^S r(i) - w(S),$$

where  $r(i)$  is the amount of exocytosis elicited by the  $i$ th action potential,  $S$  is the number of stimuli in the pool depleting train ( $S = 80$  in this case), and  $w(S)$  represents the number of vesicles that became newly available and subsequently underwent exocytosis during the stimulation.  $w(S)$  can be derived from Equation 1 (see Lemma 1) as:

$$w(S) = \sum_{i=1}^S r(i) \cdot (1 - e^{-\frac{\alpha(S-i)}{\nu}}). \quad (2A)$$

This formulation for  $w(S)$  was used to generate the *dashed line* in Figure 2A. By combining the previous two equations, we thus derive an equation for  $N$ :

$$N = \sum_{i=1}^S r(i) \cdot e^{-\frac{\alpha(S-i)}{v}}.$$

Or, by substituting  $r(1)/fe$  for  $N$ :

$$fe = \frac{r(1)}{\sum_{i=1}^S r(i) \cdot e^{-\frac{\alpha(S-i)}{v}}}. \quad (3A)$$

Equations 1A and 3A are independent because they depend on different parts of the data. Equation 3A depends on the exocytic rate during the part of the stimulation that initially depletes the RRP, whereas Equation 1A depends only on the subsequent steady-state rate of release. An analytic solution for  $\alpha$  based on Equations 1A and 3A is messy, but when the two equations are evaluated numerically using the response sizes plotted in Figure 2A as linear proxy for transmitter release, we calculate an average value for  $\alpha$  of 0.24/sec.

The simultaneous solution of Equations 1A and 3A, using the data sets plotted in Figure 2A and Figure 4,  $A_i$  and  $B_i$ , are presented graphically in Figure 2C and Figure 4,  $A_{ii}$  and  $B_{ii}$ . For each plot, the lines representing Equation 1A depend only on the steady-state response size and pass through the origin. The lines representing Equation 3A intersect the y-axis when the pool capacity is equivalent to the cumulative amount of exocytosis, because when  $\alpha = 0$ , no transmitter replenishes the pool (i.e.,  $w(S) = 0$ ). The point of intersection is taken as the common solution for  $fe$  and  $\alpha$ . A value for  $N$  can then be extracted directly by dividing the size of the first response [ $r(1)$ ] by  $fe$ .

We know from Stevens and Wesseling (1998) that  $\alpha$  is not always constant because the replenishment rate accelerates several-fold during bursts of activity. During high-frequency stimulation, however,  $\alpha(t)$  achieves its maximum value after only approximately 10 action potentials (Stevens and Wesseling, 1998). This saturation happens so quickly during 20 Hz stimulation that the required theoretical corrections to Equations 1A and 3A change the final result by a only few percentage points. By treating  $\alpha$  as a constant during high-frequency stimulation, we calculate its upper bound; the actual maximum replenishment rate is slightly slower.

### Estimates of steady-state RRP fullness predict the synaptic response settling time course caused by stimulus frequency perturbations

When the RRP is in a near-empty steady state and the stimulus frequency is suddenly doubled, as in the experiments documented in Figure 1A, the synaptic strength quickly settles to half its previous value, as expected. During the settling time, the rate of exocytosis is increased transiently, and so the 40 Hz stimulation elicits slightly more transmitter release than the corresponding 20 Hz protocol. This extra amount comes to 2.4% of the total RRP capacity calculated as above. Assuming that the pool is in a steady state at this point (i.e.,  $dn/dt = 0$ ), from Equation 1 we get a fractional fullness value (when  $n \ll N$ ) of:

$$\frac{n}{N} \approx \frac{n}{N - n} = \frac{\alpha}{\beta}.$$

If doubling the stimulus frequency also doubles  $\beta$ , the pool fullness during the 40 Hz stimulation should decline to half its steady-state value at 20 Hz. The extra amount released when the

stimulus frequency is doubled would then be equal to that half, and so at 20 Hz the fractional fullness of the RRP at steady state must be  $\sim 4.8\%$ . With this, we can solve for  $\beta$ :

$$\beta = \frac{\alpha}{0.048}.$$

For these experiments,  $\alpha = 0.25/\text{sec}$ , and so  $\beta = 5.2/\text{sec}$  during the fourth second of stimulation at 20 Hz ( $\beta = 10.4/\text{sec}$  at 40 Hz). From Equation 1 we get the general solution:

$$n = \frac{\alpha \cdot N - C \cdot e^{-t(\alpha+\beta)}}{\alpha + \beta},$$

where  $C$  is some constant that depends on the initial conditions. Perturbations in the pool fullness should thus decay back to steady state with a time constant of  $1/(\alpha + \beta)$ . In this case, the steady-state value is changed abruptly, creating an analogous situation. If our model is correct, the residual pool fullness, and thence the synaptic strength, is thus predicted to settle exponentially with a time constant of 94 msec after a sudden jump in the stimulus frequency from 20 to 40 Hz. This quantitative prediction can be seen to match well the behavior that was observed experimentally (Fig. 5, *dashed line*).

We note that this prediction depends on the specific assumption that  $\beta$  only increases twofold when the stimulus frequency is doubled. That would happen if each individual action potential triggered the exocytosis of waiting release-ready vesicles with the same efficiency during the fourth second of 20 Hz stimulation as they do when the stimulus frequency is switched instead to 40 Hz. We stress that during the first second or two of stimulation, the efficiency with which action potentials elicit exocytosis is known to increase substantially within presynaptic terminals (Stevens and Wesseling, 1999a) in a manner that depends on the stimulation frequency (Zengel and Magleby, 1982; Zucker, 1989; Delaney and Tank, 1994). Because of this frequency facilitation,  $\beta$  might be expected to more than double when the stimulus frequency is doubled in these experiments, and our estimate of the settling time course should thus be considered an upper bound estimate; that is, Equation 1 would also be consistent with a faster time course of decay. We think that the assumption is accurate, however, because we have conducted a series of studies (data not shown) that indicate that the enhancing effect of rapid stimulation on the release machinery saturates during the first several seconds of 20 Hz use at these synapses, under these conditions (unpublished observations). This also explains why it takes a similar number of action potentials to empty the RRP when the entire stimulus train is delivered at 40 Hz (half as much time) as it does when delivered at 20 Hz (Fig. 4B).

### Lemma 1: derivation of Equation 2A from Equation 1

Beginning with the assumption that Equation 1 describes the dynamics of RRP filling and emptying, consider the general case when the stimulation is initiated when the RRP is full. We can then use mathematical induction to show that  $w(S)$ , defined in Equation 2A, describes the amount of pool refilling that occurs during a stimulus train consisting of  $S$  stimuli.

#### Degenerate case

We first show that Equation 2A holds for the shortest stimulus trains consisting of only two stimuli ( $S = 2$ ). By definition, the first stimulus elicits  $r(1)$  amount of exocytosis from the RRP. No additional transmitter is released until the second stimulus elicits

the additional exocytosis of  $r(2)$  transmitter (i.e., assume that  $\beta$  in Equation 1 is equal to zero during interstimulus intervals). According to Equation 1, while  $\beta = 0$ , the empty space in the pool fills over time as:

$$w'(t) = (N - n) \cdot (1 - e^{-\alpha t}), \quad (4A)$$

where  $w'(t)$  is the amount of pool refilling over an interval during which  $\beta = 0$ ,  $t$  is time, and  $(N - n)$  is the empty space within the RRP when  $t = 0$ . Because, by assumption, the pool is full before the first stimulus, and  $r(1)$  is defined as the amount by which the RRP is diminished by the first stimulus,  $r(1) = (N - n)$  immediately after the first stimulus, but before any time has passed for pool replenishment to occur. The duration of time between the two stimuli is just the reciprocal of the stimulation rate ( $1/\nu$ ). Therefore, the amount of pool replenishment during the interval between the first and second stimuli is:

$$w'\left(\frac{1}{\nu}\right) = r(1) \cdot (1 - e^{-\frac{\alpha}{\nu}}).$$

This quantity is the amount of pool replenishment during the entire two-stimuli train because, by definition, the stimulus train ends immediately after the last stimulus, and there is no more time for additional replenishment to occur.

As defined in Equation 2A,  $w(2)$  is also equal to  $w'(1/\nu)$ :

$$w(2) = r(1) \cdot (1 - e^{-\frac{\alpha(2-1)}{\nu}}) + r(2) \cdot (1 - e^{-\frac{\alpha(2-2)}{\nu}}).$$

Because  $r(2) \cdot (1 - e^{-\frac{\alpha(2-2)}{\nu}}) = 0$ , this algebraically simplifies to:

$$w(2) = r(1) \cdot (1 - e^{-\frac{\alpha(1)}{\nu}}).$$

Equation 2A is thus at least valid for the shortest stimulus trains consisting of only two stimuli.

#### Inductive case

If we assume that Equation 2A is valid for the arbitrary case when the stimulus train consists of  $C - 1$  stimuli, we can show that the equation is also valid when the stimulus train consists of  $C$  stimuli. Assume for induction:

$$w(C - 1) = \sum_{i=1}^{C-1} r(i) \cdot (1 - e^{-\frac{\alpha(C-1-i)}{\nu}}).$$

The amount of pool replenishment that occurs during a stimulus train consisting of  $C$  stimuli is the sum of the amount occurring up to stimulus number  $C - 1$ , and the amount occurring between stimulus  $C - 1$  and stimulus  $C$ . Because the time between stimuli is  $1/\nu$ , from Equation 4A, the amount of pool replenishment between the last two stimuli must be:  $E \cdot (1 - e^{-\frac{\alpha}{\nu}})$ , where  $E$  is the total amount of free space in the RRP immediately after stimulus number  $C - 1$  ( $N - n$  in Eq. 4A). Because the amount of pool replenishment during the first  $C - 1$  stimuli of a train consisting of  $C$  stimuli must be the same as the amount of pool replenishment during the  $C - 1$  stimuli of a train consisting of only  $C - 1$  stimuli, the total pool replenishment during a train of  $C$  stimuli would be:

$$w(C) = \sum_{i=1}^{C-1} r(i) \cdot (1 - e^{-\frac{\alpha(C-1-i)}{\nu}}) + E \cdot (1 - e^{-\frac{\alpha}{\nu}}).$$

$E$  is just the difference between the transmitter release elicited by the first  $C - 1$  stimuli and the amount of pool replenishment that occurred during that time [i.e.,  $w(C - 1)$ ] and therefore can be described by:

$$E = \sum_{i=1}^{C-1} r(i) - w(C - 1).$$

Substituting for  $w(C - 1)$  and  $E$ , we have:

$$w(C) = \sum_{i=1}^{C-1} r(i) \cdot (1 - e^{-\frac{\alpha(C-1-i)}{\nu}}) + \left[ \sum_{i=1}^{C-1} r(i) - \sum_{i=1}^{C-1} r(i) \cdot (1 - e^{-\frac{\alpha(C-1-i)}{\nu}}) \right] \cdot (1 - e^{-\frac{\alpha}{\nu}}).$$

This simplifies algebraically to:

$$w(C) = \sum_{i=1}^{C-1} r(i) \cdot (1 - e^{-\frac{\alpha(C-i)}{\nu}}).$$

And, because  $r(C) \cdot (1 - e^{-\frac{\alpha(C-C)}{\nu}}) = 0$ , we conclude that Equation 2A is valid for a stimulus train of  $C$  stimuli:

$$w(C) = \sum_{i=1}^C r(i) \cdot (1 - e^{-\frac{\alpha(C-i)}{\nu}}).$$

We have thus shown that if Equation 2A is valid for a stimulus train of arbitrary length, then the equation must also be valid for a train that is longer by a single stimulus. Because we also showed that Equation 2A is valid for the shortest trains consisting of only two stimuli, it must also be true for trains of length 3, 4, and so on for trains of any length by the principle of mathematical induction. Taken together, this logic demonstrates that Equation 2A follows from Equation 1 in all cases.

#### REFERENCES

- Abbott LF, Varela JA, Sen K, Nelson SB (1997) Synaptic depression and cortical gain control. *Science* 275:220–224.
- Allen C, Stevens CF (1994) An evaluation of causes for unreliability of synaptic transmission. *Proc Natl Acad Sci USA* 91:10380–10383.
- Asztely F, Erdemli G, Kullmann DM (1997) Extrasynaptic glutamate spillover in the hippocampus: dependence on temperature and the role of active glutamate uptake. *Neuron* 18:281–293.
- Auger C, Marty A (2000) Quantal currents at single-site central synapses. *J Physiol (Lond)* 526:3–11.
- Beutner D, Voets T, Neher E, Moser T (2001) Calcium dependence of exocytosis and endocytosis at the cochlear inner hair cell afferent synapse. *Neuron* 29:681–690.
- Birks RI, MacIntosh FC (1961) Acetylcholine metabolism of a sympathetic ganglion. *Can J Biochem Physiol* 39:787–827.
- Curtis DR, Eccles JC (1960) Synaptic action during and after repetitive stimulation. *J Physiol (Lond)* 150:374–398.
- Delaney KR, Tank DW (1994) A quantitative measurement of the dependence of short-term synaptic enhancement on presynaptic residual calcium. *J Neurosci* 14:5885–5902.
- Diamond JS, Jahr CE (1997) Transporters buffer synaptically released glutamate on a submillisecond time scale. *J Neurosci* 17:4672–4687.
- Dittman JS, Regehr WG (1998) Calcium dependence and recovery kinetics of presynaptic depression at the climbing fiber to Purkinje cell synapse. *J Neurosci* 18:6147–6162.
- Dobrunz LE, Stevens CF (1997) Heterogeneity of release probability, facilitation, and depletion at central synapses. *Neuron* 18:995–1008.
- Eccles JC, Rall W (1951) Repetitive monosynaptic activation of motoneurons. *Proc R Soc Lond B Biol Sci* 138:475–498.
- Elmqvist D, Quastel DM (1965) A quantitative study of end-plate potentials in isolated human muscle. *J Physiol (Lond)* 178:505–529.

- Frakenhaeuser B, Hodgkin AL (1957) The action of calcium on the electrical properties of squid axons. *J Physiol (Lond)* 137:218–244.
- Hessler NA, Shirke AM, Malinow R (1993) The probability of transmitter release at a mammalian central synapse. *Nature* 366:569–572.
- Huang EP, Stevens CF (1997) Estimating the distribution of synaptic reliabilities. *J Neurophysiol* 78:2870–2880.
- Jonas P, Major G, Sakmann B (1993) Quantal components of unitary EPSCs at the mossy fibre synapse on CA3 pyramidal cells of rat hippocampus. *J Physiol (Lond)* 472:615–663.
- Kawasaki F, Mattiuz AM, Ordway RW (1998) Synaptic physiology and ultrastructure in comatose mutants define an *in vivo* role for NSF in neurotransmitter release. *J Neurosci* 18:10241–10249.
- Knierim JJ, van Essen DC (1992) Neuronal responses to static texture patterns in area V1 of the alert macaque monkey. *J Neurophysiol* 67:961–980.
- Kusano K, Landau EM (1975) Depression and recovery of transmission at the squid giant synapse. *J Physiol (Lond)* 245:13–22.
- Liu G, Choi S, Tsien RW (1999) Variability of neurotransmitter concentration and nonsaturation of postsynaptic AMPA receptors at synapses in hippocampal cultures and slices. *Neuron* 22:395–409.
- McAllister AK, Stevens CF (2000) Nonsaturation of AMPA and NMDA receptors at hippocampal synapses. *Proc Natl Acad Sci USA* 97:6173–6178.
- Meister M, Berry II MJ (1999) The neural code of the retina. *Neuron* 22:435–450.
- Murthy VN, Stevens CF (1999) Reversal of synaptic vesicle docking at central synapses. *Nat Neurosci* 2:503–507.
- Neher E, Sakaba T (2001) Combining deconvolution and noise analysis for the estimation of transmitter release rates at the calyx of held. *J Neurosci* 21:444–461.
- Neher E, Zucker RS (1993) Multiple calcium-dependent processes related to secretion in bovine chromaffin cells. *Neuron* 10:21–30.
- Newsome WT, Britten KH, Movshon JA (1989) Neuronal correlates of a perceptual decision. *Nature* 341:52–54.
- Patneau DK, Vyklicky Jr L, Mayer ML (1993) Hippocampal neurons exhibit cyclothiazide-sensitive rapidly desensitizing responses to kainate. *J Neurosci* 13:3496–3509.
- Pyle JL, Kavalali ET, Piedras-Renteria ES, Tsien RW (2000) Rapid reuse of readily releasable pool vesicles at hippocampal synapses. *Neuron* 28:221–231.
- Pyott SJ, Rosenmund C (2002) . The effects of temperature on vesicular supply and release in autaptic cultures of rat and mouse hippocampal neurons. *J Physiol (Lond)* 539:523–535.
- Ranck Jr JB (1973) Studies on single neurons in dorsal hippocampal formation and septum in unrestrained rats. I. Behavioral correlates and firing repertoires. *Exp Neurol* 41:462–531.
- Rosenmund C, Stevens CF (1996) Definition of the readily releasable pool of vesicles at hippocampal synapses. *Neuron* 16:1197–1207.
- Rosenmund C, Clements JD, Westbrook GL (1993) Nonuniform probability of glutamate release at a hippocampal synapse. *Science* 262:754–757.
- Sakaba T, Neher E (2001) Quantitative relationship between transmitter release and calcium current at the calyx of Held synapse. *J Neurosci* 21:462–476.
- Schikorski T, Stevens CF (1997) Quantitative ultrastructural analysis of hippocampal excitatory synapses. *J Neurosci* 17:5858–5867.
- Schikorski T, Stevens CF (2001) Morphological correlates of functionally defined synaptic vesicle populations. *Nat Neurosci* 4:391–395.
- Scott TR, Yaxley S, Sienkiewicz ZJ, Rolls ET (1986) Gustatory responses in the nucleus tractus solitarius of the alert cynomolgus monkey. *J Neurophysiol* 55:182–200.
- Stevens CF, Tsujimoto T (1995) Estimates for the pool size of releasable quanta at a single central synapse and for the time required to refill the pool. *Proc Natl Acad Sci USA* 92:846–849.
- Stevens CF, Wesseling JF (1998) Activity-dependent modulation of the rate at which synaptic vesicles become available to undergo exocytosis. *Neuron* 21:415–424.
- Stevens CF, Wesseling JF (1999a) Augmentation is a potentiation of the exocytotic process. *Neuron* 22:139–146.
- Stevens CF, Wesseling JF (1999b) Identification of a novel process limiting the rate of synaptic vesicle cycling at hippocampal synapses. *Neuron* 24:1017–1028.
- Sudhof TC (1995) The synaptic vesicle cycle: a cascade of protein-protein interactions. *Nature* 375:645–653.
- Trussell LO, Zhang S, Raman IM (1993) Desensitization of AMPA receptors on multiquantal neurotransmitter release. *Neuron* 10:1185–1196.
- Tsodyks MV, Markram H (1997) The neural code between neocortical pyramidal neurons depends on neurotransmitter release probability. *Proc Natl Acad Sci USA* 94:719–723.
- Voets T (2000) Dissection of three Ca<sup>2+</sup>-dependent steps leading to secretion in chromaffin cells from mouse adrenal slices. *Neuron* 28:537–545.
- Voets T, Neher E, Moser T (1999) Mechanisms underlying phasic and sustained secretion in chromaffin cells from mouse adrenal slices. *Neuron* 23:607–615.
- Wang LY, Kaczmarek LK (1998) High-frequency firing helps replenish the readily releasable pool of synaptic vesicles. *Nature* 394:384–388.
- Wu LG, Borst JG (1999) The reduced release probability of releasable vesicles during recovery from short-term synaptic depression. *Neuron* 23:821–832.
- Yamada KA, Tang CM (1993) Benzothiadiazides inhibit rapid glutamate receptor desensitization and enhance glutamatergic synaptic currents. *J Neurosci* 13:3904–3915.
- Zengel JE, Magleby KL (1982) Augmentation and facilitation of transmitter release. A quantitative description at the frog neuromuscular junction. *J Gen Physiol* 80:583–611.
- Zucker RS (1973) Changes in the statistics of transmitter release during facilitation. *J Physiol (Lond)* 229:787–810.
- Zucker RS (1989) Short-term synaptic plasticity. *Annu Rev Neurosci* 12:13–31.